6031

A Numerical Prediction of Thermal Environment In a Room Heated with Floor Panels

M. KAIZUKA
Professor,
Dept. of Architecture,
School of Engineering and
Technology, Meiji University
Kawasaki-shi, 214 Japan

S. IWAMOTO
Research Associate,
Dept. of Environmental
Design, Faculty of Design,
Kyushu Institute of Design
Fukuoka-shi, 815 Japan

A. ISHII
Professor,
Dept. of Environmental
Design, Faculty of Design,
Kyushu Institute of Design
Fukuoka-shi, 815 Japan

ABSTRACT

This paper presents a numerical prediction method and predicted results of steady state distribution of thermal environment in a room heated with hot water floor panels. Natural buoyant air flow was predicted with the k-ε turbulence model combined with heat transfer through walls and radiation exchanges on wall surfaces. Then, thermal comfort indexes, PMV and SET were calculated to illustrate characteristics of thermal environment.

KEYWORDS Numerical simulation, Natural convection, Radiation, Thermal comfort, Floor heating

1. INTRODUCTION

For adequate evaluation and design of indoor thermal environment, it is helpful to predict distribution of such variables as air movement, air temperature, wall surface temperature, mean radiant temperature and thermal comfort index. This paper presents a numerical method developed for a simulation of the above described variables and results of an application of this method to a test room which was constructed inside the weather controlled laboratory and heated with hot water floor panels. The following points are specifically emphasized as the targets of the present study.

- To establish a steady state solution method with favorable convergence stability for natural convection field.
- To combine radiation effect on surface temperature and thermal comfort index with room air convection.
- To grasp the characteristics of indoor thermal environment with floor heating.

2. ROOM CONFIGURATION AND CONDITIONS

Figure 1 shows the room plan to simulate thermal environment in this study. A box-shaped room with width of 3.6m, depth of 3.6m, and height of 2.4m was built inside the weather controlled laboratory for a test of heating appliances. Most of the room floor indicated by the dotted lines in the figure had hot water piped heating panels beneath the flooring board. The temperatures of the heated floor surface, of the air in the room neighboring to the east and of the outdoor air were set at 34.0, 10.0 and 3.5℃ respectively. Thermal conductances of the walls from inside surface to outside air were set at the given values. Details of the wall components may be found in Iwamoto and Kaizuka (1990).

For thermal conduction in the walls, one dimensional heat flow was assumed, without considering three dimensional heat flow at the corner sections and heat bridges around the sashes. For thermal radiation, the exchanges between the wall

surfaces assuming perfect diffusion were considered with the emissivity of 0.9 without considering solar radiation through the windows and mirror reflection effect. It was assumed that neither ventilation, heat generating apparatus nor furniture is existed. These assumptions were adopted simplifying prediction procedures, but a proper modeling will be required for more realistic prediction.

For the calculation of surface temperature distribution, the room surface was divided into 82 surface sections of approximately 70cmx70cm each. For the calculation of air convection, the room space was divided into 41x40x30 cells with nonuniform layout patterns of varying intervals between cells; 2cm near the wall and 13cm at the center.

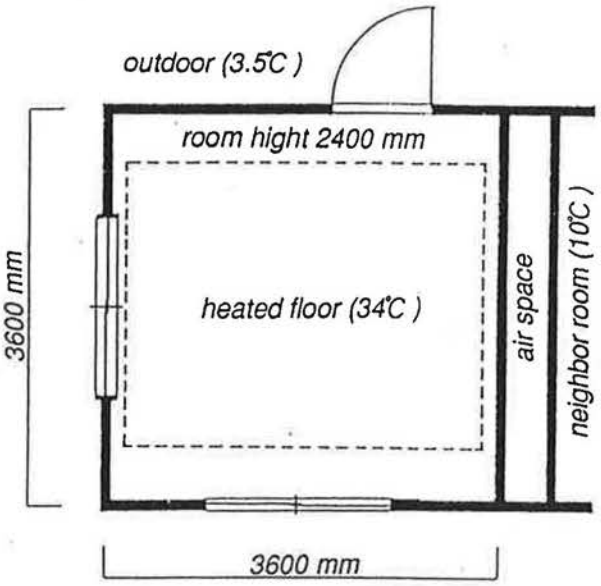

Figure 1 Room Plan

3. METHOD OF PREDICTION

As shown in Figure 2, the calculation methods below are used in combination.

3.1 Flow Field

The k-ε turbulence model (Launder and Spalding 1972) is transformed into Equations (1)-(6) as shown in Table 1, and the steady state solving method developed by Matsuo(1986) with conjugate gradient method (CGM) and the source term linearization (Patankar 1980) is applied. The empirical constant C_3 is derived from the study result by Mochida et al.(1988). For the finite difference method, the staggered arrangement of variables (Harlow and Welch 1965), QUICK scheme (Leonard 1979) to the momentum equation and the upwind scheme to the scalar equations are used. The wall functions adopted are indicated in Equations (7)-(10) as shown in Table 2 utilizing the Karman's three layer model. Details of the calculation method may be found in Kaizuka and Iwamoto (1989) and Kurabuchi et al.(1988).

3.2 Wall Surface Temperature

For determining surface temperature of each element T_i , Equation (11) for thermal balance based on conduction, convection and radiation is applied as shown in Table 3 (Sakamoto 1977).

The conduction heat flux is expressed by the

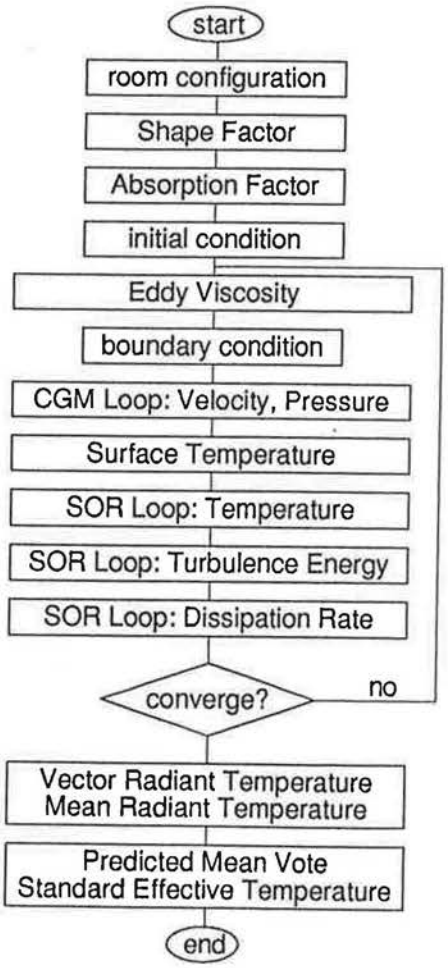

Figure 2 Flow Chart for Calculation

given thermal conductance C_I, the given outside air temperature and T_I as shown in Equation (12). The convection heat flux is obtained by averaging the values from Equation (8) for all cells contacting the surface element as shown in Equation (13). For the calculation of radiation exchanges, the shape factors between surface elements are calculated using the method developed by Yamazaki (1983), and the simultaneous linear equation of the absorption factor (Gebhart 1959) is solved. With these, the net radiation heat flux received is expressed by Equation (14), then approximated to the linear form of temperature difference using the reciprocity theorem and mean temperature.

The simultaneous linear equation of T_I thus obtained by Equations (11)-(14) is solved directly with the LU decomposition method. This procedure is taken into the iteration loop of the prediction to use for the boundary condition of the surface temperature as shown in Figure 2.

3.3 Mean and Vector Radiant Temperature

In order to grasp the distribution of radiation field in an indoor space, the mean radiant temperature and vector radiant temperature proposed by Nakamura (1987) are calculated. 7x7x6 orthogonal grid points are set in the room with horizontal intervals of 50cm and vertical intervals of 40cm. An infinitely small cube as shown in Table 4 is assumed at every grid point, and the mean radiant temperature for each of the six surfaces is calculated with Equation (15). This temperature stands for the temperature of an imaginary black body surrounding the surface, and the radiation heat flux from the black body to the surface is equal to that from the real indoor surfaces. The average of the mean radiant temperature of the six surfaces expressed by Equation (16) is the mean radiant temperature at the point in question, and it represents the index showing the radiation heat flux intensity from the room surface to that point. The vector with the component of the directional difference of the mean radiant temperature of the infinitely small cube represented by Equation (17) is a vector radiant temperature, which is the index showing the direction of a radiation field.

Table 1 Basic Equations

$$\frac{\partial u_j}{\partial x_j}=0 \tag{1}$$

$$\frac{\partial u_j^* u_i}{\partial x_j}=-\frac{\partial \Pi}{\partial x_i}+\frac{\partial}{\partial x_j}\left\{\nu_e\left(\frac{\partial u_i}{\partial x_j}+\frac{\partial u_j}{\partial x_i}\right)\right\}+\delta_{i3}\theta \tag{2}$$

$$\frac{\partial u_j^* \theta}{\partial x_j}=\frac{\partial}{\partial x_j}\left(\nu_\theta \frac{\partial \theta}{\partial x_j}\right) \tag{3}$$

$$\frac{\partial u_j^* k}{\partial x_j}=\frac{\partial}{\partial x_j}\left(\nu_k \frac{\partial k}{\partial x_j}\right)+P_k^*-\frac{\varepsilon^*}{k^*}k+G_k^* \tag{4}$$

$$\frac{\partial u_j^* \varepsilon}{\partial x_j}=\frac{\partial}{\partial x_j}\left(\nu_\varepsilon \frac{\partial \varepsilon}{\partial x_j}\right)+\frac{\varepsilon^*}{k^*}(C_1 P_k^*-C_2\varepsilon+C_3 G_k^*) \tag{5}$$

$$\nu_t=C_D\frac{k^2}{\varepsilon} \tag{6}$$

$$\Pi=\frac{p}{\rho}+\frac{2}{3}k,\quad P_k=\nu_t\left(\frac{\partial u_i}{\partial x_j}+\frac{\partial u_j}{\partial x_i}\right)\frac{\partial u_i}{\partial x_j},\quad G_k=-\frac{\nu_t}{\sigma_\theta}\frac{\partial \theta}{\partial x_3}$$

$$\nu_e=\nu+\nu_t,\quad \nu_\theta=\frac{\nu}{\sigma}+\frac{\nu_t}{\sigma_\theta},\quad \nu_k=\nu+\frac{\nu_t}{\sigma_k},\quad \nu_\varepsilon=\nu+\frac{\nu_t}{\sigma_\varepsilon}$$

$$\sigma_\theta=0.7,\quad \sigma_k=1.0,\quad \sigma_\varepsilon=1.3$$

$$C_D=0.09,\quad C_1=1.44,\quad C_2=1.92,\quad C_3=\begin{cases}0 & (\partial\theta/\partial x_3>0)\\ C_1 & (\partial\theta/\partial x_3<0)\end{cases}$$

x_i: *space coordinate* ν_t: *eddy kinematic viscosity*
u_i: *velocity* $\sigma_\square$: *Prandtl number*
p: *excess pressure* $C_\square$: *empirical constant*
θ: *temperature* $\square^*$: *former value in iteration*
k: *turbulence energy* $\square_o$: *representative scale*
ε: *dissipation rate* $L_o=1m,\ \Delta\theta_o=34℃$
ν: *kinematic viscosity* $U_o\equiv\sqrt{g\beta\Delta\theta_o L_o}=1.1m/s$

Table 2 Wall Boundary Condition

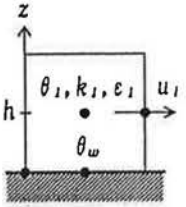

$$\left(\nu_e\frac{\partial u}{\partial z}\right)_w=\frac{u_1 C_D^{1/4}k_1^{1/2}}{f(R_h)} \tag{7}$$

$$\left(\nu_\theta\frac{\partial \theta}{\partial z}\right)_w=\frac{\theta_1-\theta_w}{\sigma_\theta}\frac{C_D^{1/4}k_1^{1/2}}{f(R_h)} \tag{8}$$

$$\left(\frac{\partial k}{\partial z}\right)_w=0 \tag{9}$$

$$\varepsilon_1=\frac{C_D^{3/4}k_1^{3/2}}{\kappa h} \tag{10}$$

$$R_h=\frac{C_D^{1/4}k_1^{1/2}h}{\nu},\quad f(R_h)=\begin{cases}R_h & 0<R_h<5\\ 5\ell nR_h-3.05 & 0<R_h<30\\ 2.5\ell nR_h+5.5 & 30<R_h\end{cases}$$

κ: *von Karman constant* 0.4

3.4 Thermal Comfort Index

The distribution of the representative thermal comfort indexes, Predicted Mean Vote by Fanger (1972) and Standard Effective Temperature by Gagge et al. (1976) were calculated. Both of them are the function of six variables, air temperature, mean radiant temperature, air flow velocity, humidity, clothing and thermal metabolic rate.

Here the clothing is set to 1clo (business suit), metabolic rate 1met (sedentary) and water vapor pressure 7mmHg (40% at 20℃) uniformly. An equation for convection and diffusion may have to be employed for the consideration of the distribution of water vapor, but here it is assumed uniform as it may little affect the thermal comfort in heating. The air temperature and airflow velocity obtained from the calculation of flow fields were used.

The mean radiant temperature for a person of averaged direction was calculated following Nakamura (1987) as shown in Table 5. The shape factor for a person is approximated by multiplying weighting factors by the shape factors for six surfaces of the infinitely small cube as expressed in Equation (18). Or it can also be indicated by approximating the mean radiant temperature for a person with an infinitely small box of nearly 1:1:2 for seated position and nearly 1:1:10 for standing position.

4. RESULTS AND DISCUSSION

Stably converged results were obtained with the above mentioned prediction method, by uniformly setting the initial values of u, v, w and p at 0, and the room surface and air temperature at the outdoor air temperature. The results are illustrated as shown in the following figures utilizing the visualization algorithm developed by Mr. M. Sato (Kajima Corporation).

4.1 Room Air Convection

The path lines of markers located with equal intervals on the cross-sectional area are shown in Figure 3. In Figure 4, the path lines of markers randomly generated that pass through a light sheet are shown, which is simulating the visualization of

Table 3 Heat Balance on Surface

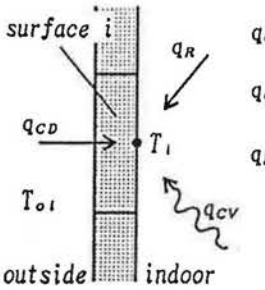

$$q_{CD} + q_{CV} + q_R = 0 \quad (11)$$

$$q_{CD} = C_i (T_{oi} - T_i) \quad (12)$$

$$q_{CV} = c_p \rho \left(\nu_\theta \frac{\partial \theta}{\partial n}\right)_w \quad (13)$$

$$q_R = \sigma \left(\sum_j \varepsilon_j B_{ji} T_j^4 - \varepsilon_i T_i^4\right) \quad (14)$$

$$\fallingdotseq 4 T_m^3 \sigma \varepsilon_i \sum_j B_{ij} (T_j - T_i)$$

c_p : specific heat of air
σ : Stefan-Boltzmann constant
ε_i : emissivity of surface i
B_{ij} : Gebhart's absorption factor
q_{CD} : conduction heat flux from wall to i surface
q_{CV} : convection heat flux from cell on i surface
q_R : net radiation heat flux to i surface
C_i : wall conductance from outside air to i surface
T_i : temperature of i surface (absolute)
T_{oi} : temperature of outside air (absolute)
T_m : mean temperature (absolute)

Table 4 Mean and Vector Radiant Temperature

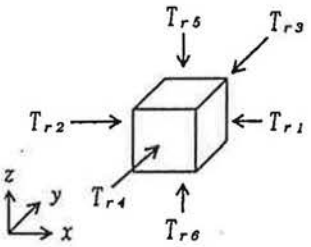

T_{rb} :MRT of b surface
T_{mrt} :MRT of a cube
ϕ_{bi} :shape factor of i surface to b
Θ :vector radiant temperature
$\mathbf{i}, \mathbf{j}, \mathbf{k}$:unit vector

$$\sigma T_{rb}^4 = \sum_i \phi_{bi} \left\{ \varepsilon_i \sigma T_i^4 + \frac{1-\varepsilon_i}{\varepsilon_i} \sum_j \sigma \varepsilon_j B_{ji} T_j^4 \right\} \quad (15)$$

$$T_{mrt} = \frac{1}{6} \sum_{b=1}^{6} T_{rb} \quad (16)$$

$$\Theta = (T_{r2} - T_{r1})\,\mathbf{i} + (T_{r4} - T_{r3})\,\mathbf{j} + (T_{r6} - T_{r5})\,\mathbf{k} \quad (17)$$

Table 5 Shape Factor and MRT for a Person

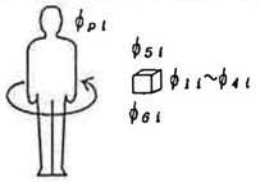

ϕ_{pi} :shape factor of i to a person
ϕ_{bi} :shape factor of i to b of a cube
T_{pmrt} :MRT of a person

$$\phi_{pi} = \sum_{b=1}^{6} a_b \phi_{bi} \quad (18)$$

$$\sigma T_{pmrt}^4 = \sum_i \phi_{pi} \left\{ \varepsilon_i \sigma T_i^4 + \frac{1-\varepsilon_i}{\varepsilon_i} \sum_j \varepsilon_j \sigma B_{ji} T_j^4 \right\} \quad (19)$$

a_b:weighting factor for each surface of a cube

	horizontal a_5, a_6	vertical $a_1 \sim a_4$
seated	0.102	0.199
standing	0.024	0.238

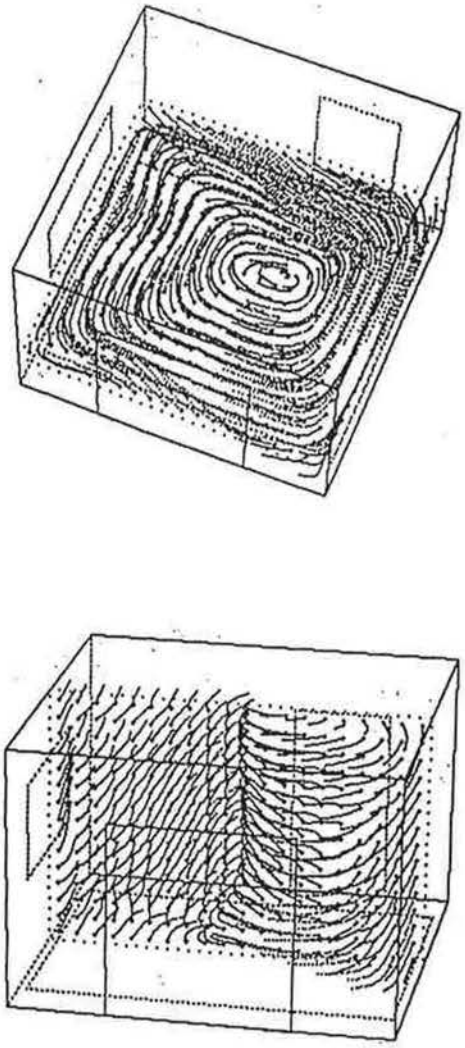

Figure 3 Paths of Regular Markers

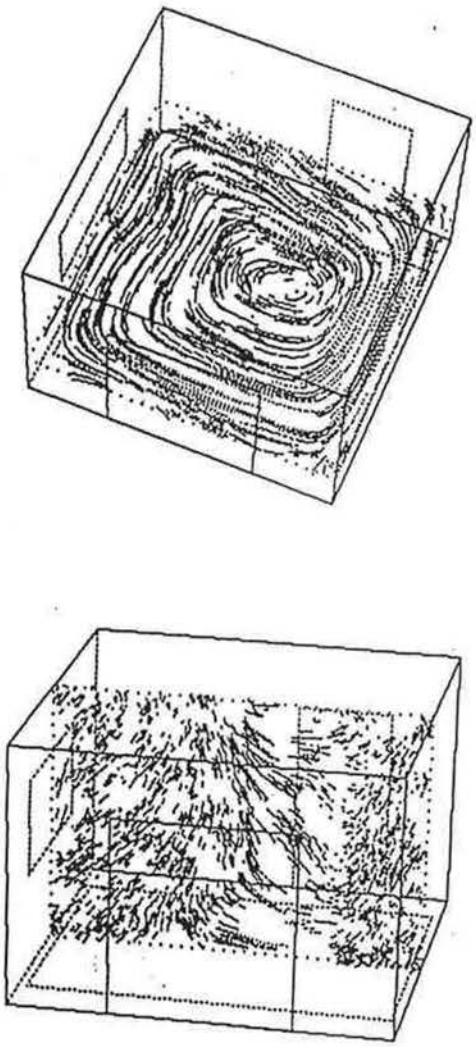

Figure 4 Paths of Random Markers

tracer particles with a laser light sheet. The vertical cross-sectional area is located at the center of the room, and the horizontal cross-sectional area at 0.6m above the floor. From these figures, a horizontally circulating flow covering the entire room and a buoyant plume upward at the central part of the room can be seen clearly. The total airflow pattern, however, is three dimensional and considerably complicated for easy description. The airflow velocity is less than 0.13m/s and can be regarded as almost still air.

Figure 5 shows the excess pressure from the outdoor pressure of same height. It is distributed horizontally in layer with a constant gradient mostly without disturbance, which would be considered reasonable in this type of natural convection.

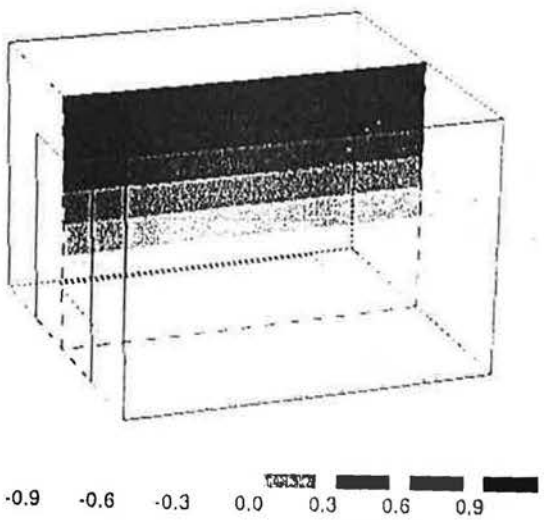

Figure 5 Pressure p (Pa)

4.2 Turbulence Properties

Figure 6, 7, and 8 show the distribution of turbulence energy k, dissipation rate ε and eddy viscosity ν_t respectively. Developed turbulence was observed in the entire room, and high values of k and ν_t were seen at the room center, and ε near the floor surface.

4.3 Room Air Temperature

Figure 9 shows the cross sectional distribution of the room air temperature. While the average temperature is 23.5℃, near the floor of the central part it shows higher temperature. Near the windows and the exterior walls lower temperature caused by the down draft from the cold surfaces can be seen. This down draft, however, is not obviously seen in Figure 3 or Figure 4. This is due to the fact that the figures are illustrated based on the extrapolated coarse mesh data. The original fine mesh data clearly shows the down draft.

4.4 Mean and Vector Radiant Temperature

Figure 10 shows the distribution of the mean radiant temperature of the infinitely small cube. A little higher gradient than that of the room air temperature is seen from the floor surface toward the ceiling surface, and it lowers toward the windows.

Figure 11 shows the vector radiant temperature. The radiation flow from the floor surface can be seen clearly, and the highest value of 13℃ produced by the flow is seen toward the terrace window.

4.5 Distribution of PMV and SET

Figure 12 and 13 show the horizontal distribution of PMV and SET for seated position. Their values are higher toward the central part of the room and lower toward the windows and exterior walls, and the shapes of the distribution are well in agreement. The averaged value of PMV is -0.03 and that of SET is 25.1℃, both of them are considered almost neutral or comfortable.

4.6 Comparison with Measurement

Although experimental data to validate the pre-

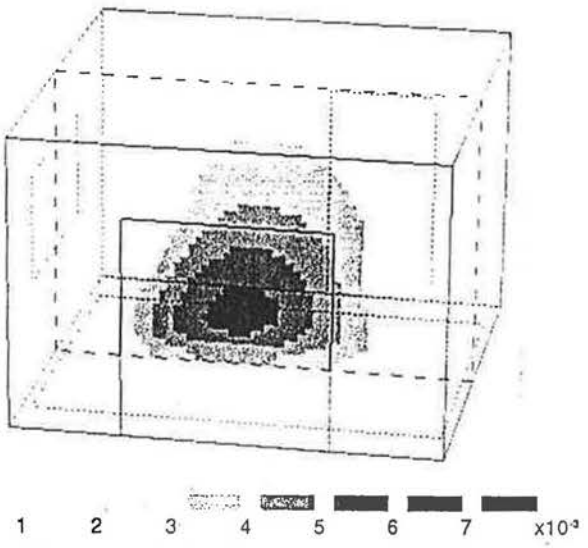

Figure 6 Turbulence Energy k (m^2/s^2)

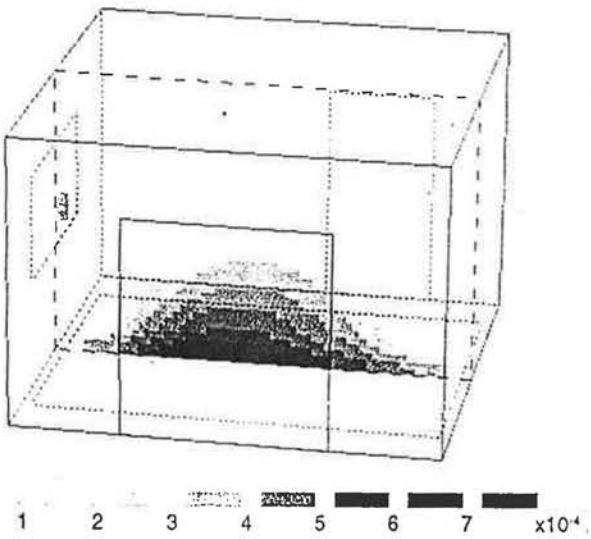

Figure 7 Dissipation Rate ε (m^2/s^3)

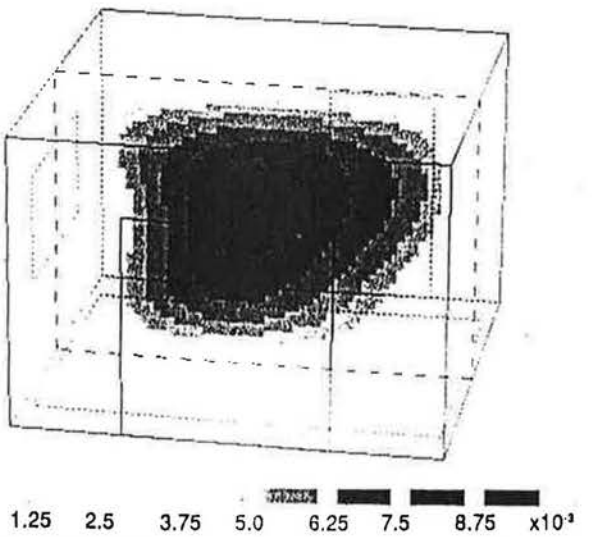

Figure 8 Eddy Kinematic Viscosity ν_t (m^2/s)

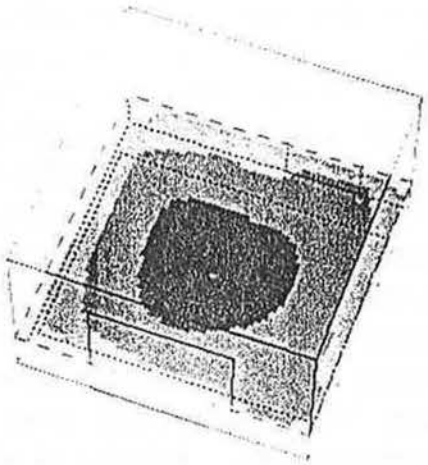

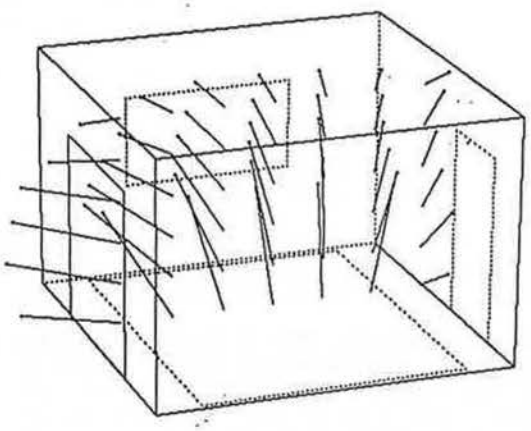

Figure 11 Vector Radiant Temperature Θ (C)

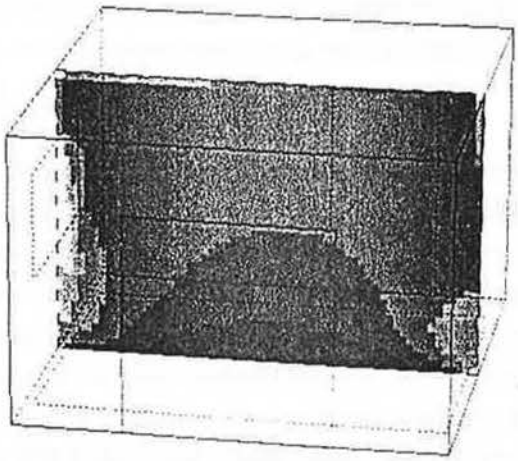

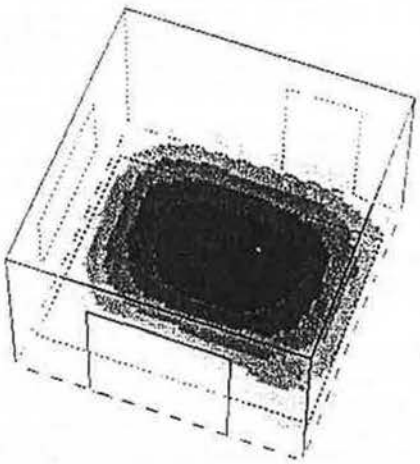

19 20 21 22 23 24 25 ℃

Figure 9 Air Temperature θ (C)

-0.3 -0.2 -0.1 0.0 0.1 0.2 0.3

Figure 12 Predicted Mean Vote

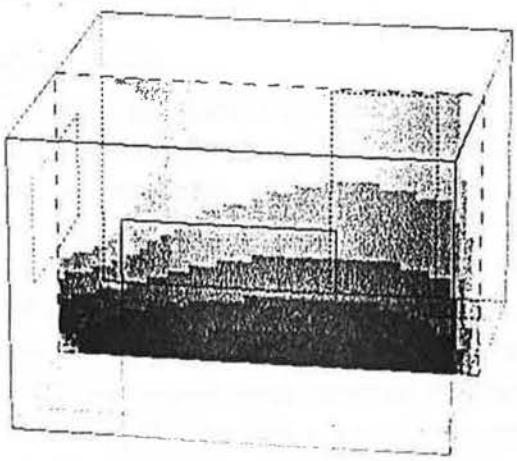

20 21 22 23 24 25 26 ℃

Figure 10 Mean Radiant Temperature T_{mrt} (C)

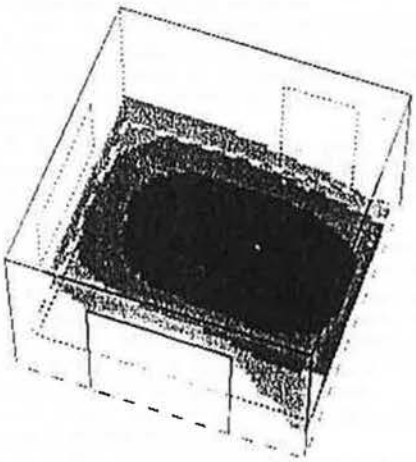

23.5 24.0 24.5 25.0 25.5 26.0 26.5 ℃

Figure 13 Standard Effective Temperature (C)